Effects of Slab Post-Tensioning on Supporting Steel Beams in Steel Framed Parking Deck Structures

BHAVNA SHARMA and KENT A. HARRIES

AISC Design Guide 18, *Steel-Framed Open-Deck Parking Structures* (Churches, Troop and Angelof, 2003), discusses the use of cast-in-place post-tensioned concrete slabs in steel-framed parking structures. In Section 3.3.2.1 of Design Guide 18, the authors reflect on the manner in which the post-tensioning force is resisted by and affects the supporting beam: in a noncomposite or composite manner. They conclude that the post-tensioning force is carried almost entirely in a composite manner (minus effects of shrinkage and elastic shortening). This conclusion is based on results of unpublished research and is corroborated by earlier design guidance provided by Bakota (1988). The objective of this field study is to quantitatively assess the effect that slab post-tensioning forces have on their supporting steel members.

CURRENT PRACTICE

Cast-in-place post-tensioned concrete slabs on steel girders are an attractive alternative for parking structures. The use of post-tensioned (PT) slabs permits somewhat longer spans to be achieved than for non-PT slabs but primarily enhances the durability of the slab system, affecting superior crack control and improved negative moment region behavior. Investigation of the effects of the post-tensioning stress on the composite behavior of the beams has been explored but not published. Current practice, as promulgated in AISC Design Guide 18 (Churches et al., 2003) assumes that the composite beams experience a small amount of compressive stress from the post-tensioning of the slab. Design Guide 18 notes that unpublished testing by Mulach Steel Corporation demonstrated a "stress increase of 3% in the composite beams under dead load conditions." Discussion of these tests with Churches (2007) indicated that this increase is the net additional tensile stress in the tension flange of the beam associated with the combination of PT-induced flexure (tension) and PT-induced axial (compression) forces.

Bakota (1988) explores the design of a post-tensioned parking deck and analyzes the effects of post-tension stresses on the composite beam. The author notes various design criteria for a post-tensioned deck and that an effective post-tension stress of 100 psi in the transverse shrinkage and temperature direction reduces the effects of the post-tensioning parallel to the beam. Bakota presents equations to determine the long-term stresses and deflections. He concludes that the post-tension forces in the deck create long-term beam and slab stresses due to differential volume changes.

Steel-framed parking structures, in general, were introduced in the literature in the 1970s (Sontag, 1970; AISC, 1974). Frequent references and case studies appear in the literature through today: in North America, typically appearing in *Modern Steel Construction*; in Europe, in *Acier-Stahl-Steel*; and elsewhere including a number of references in the South African Journal, *Steel Construction*. In addition to Design Guide 18, AISC promulgates *Innovative Solution in Steel: Open Deck Parking Structures* (Troup and Cross, 2003). Available references in the literature primarily address precast concrete decks on steel frames (Simon, 2001; Englot and Davidson, 2001; Flynn and Astaneh-Asl, 2001). A review of available literature revealed no additional publications relating specifically to cast-in-place post-tensioned concrete decks on steel frames.

TEST STRUCTURE

To investigate the effects of post-tensioning the concrete deck on the steel structure, a candidate test structure was selected, instrumented and monitored through its construction and initial service (Sharma and Harries, 2007). All reported testing-related activities were carried out between November 10, 2006, and January 12, 2007. The test structure is a single-story steel parking structure having a post-tensioned composite concrete deck. The structure, shown in Figure 1, is a single-story steel frame over a slab on-grade. Parking is provided on both levels, although there is no connecting ramp. Separate entrances are provided for the grade and deck parking.

As shown in Figure 2, the structure has 11 bays (10 measuring 20 ft and the first measuring 15 ft) in the north-south (N-S) direction and two bays in the east-west (E-W)

Bhavna Sharma is a Ph.D. and IGERT Fellow candidate at the University of Pittsburgh, Pittsburgh, PA.

Kent A. Harries is an assistant professor, University of Pittsburgh, Pittsburgh, PA.

direction: bay 1-2, measuring 45 ft 2 in., and bay 2-3, measuring 35 ft 2 in. There is a 10-ft cantilever beyond column line 3. All columns are W12×65 and the beams spanning bay 1-2 are W24×76 at beams C and D and W24×68 at beam B. Where beams frame into girders, a simple full-depth double-angle shear connection is provided. Beams that frame into columns (all strong axis for the beams considered in this study) are provided with angles at both top and bottom flanges, resulting in a partially-restrained connection. The beams considered in this study span bay 1-2 at column lines B, C and D and are referred to as beams B, C and D, respectively, as indicated in Figure 2. The span of the structure considered is approximately 45 ft and is not necessarily representative of a typical steel-framed parking structure, which often span approximately 60 ft. Nonetheless, all elements are proportional and thus the conclusions drawn based on the 45-ft span are believed to be representative.

The cast-in-place concrete deck is a 6-in. post-tensioned concrete slab. Reinforcing details of the deck are shown in Figure 3. Single, double and triple strands are arranged as shown in Figure 2b. All strands have their anchorages centered in the 6-in. deck depth. The concrete stress due to initial post tensioning is 330 psi in the N-S direction and 168 psi in the E-W direction. Mild steel is arranged primarily

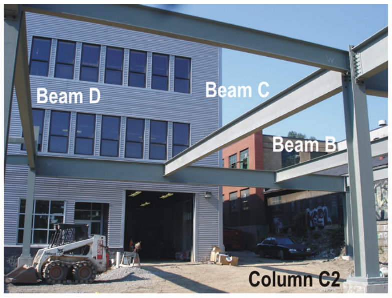

(a) Beams B, C and D during erection.


(b) Deck prior to concrete placement.

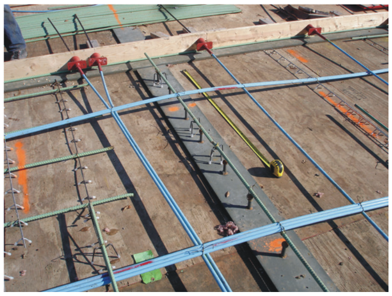
(c) Beam B at girder 2.


(d) Concrete placement.


(e) Pulling PT strand near beam A.


(f) Completed structure looking North; beams B, C and D in far background.

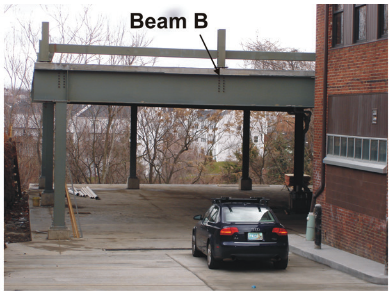

(g) Completed structure looking East showing beams A and B.

Fig. 1. Test structure.

for crack control as indicated in Figure 3. Additionally, ⅝ × 3 in. shear studs are provided along all beams in bay 1-2 at a spacing of 10 in. as shown in Figure 1c.

Materials

All structural steel members considered in this study are ASTM A992 Grade 50. No material tests were conducted on this steel. The specified concrete compressive strength was 5,000 psi. Both the University of Pittsburgh team and the contractor placed test cylinders. The 28-day concrete compressive strength was determined to be 5,100 psi and the 5-day strength (at the time of pulling the PT strand) was 3,450 psi. All post-tensioning strands used in the deck were ½-in., 270-ksi, seven-wire prestressing strands (A_{ps} = 0.153 in.^{2}). The strand was enclosed in a greased plastic sheath. All mild reinforcement in the deck is #5 epoxy-coated reinforcing bar having a nominal yield strength of f_y = 60 ksi. No material tests were conducted on any of the steel reinforcement. The mild steel was provided only for crack control and is not sufficient to affect the deck structural behavior.

Instrumentation

Electrical resistance strain gauges were installed on beams B, C and D. As shown in Figure 4, gauges were located at five sections along beams B and D and at three sections along beam C. At each section, three gauges were provided as shown in Figure 4b: one on the bottom of the top flange,

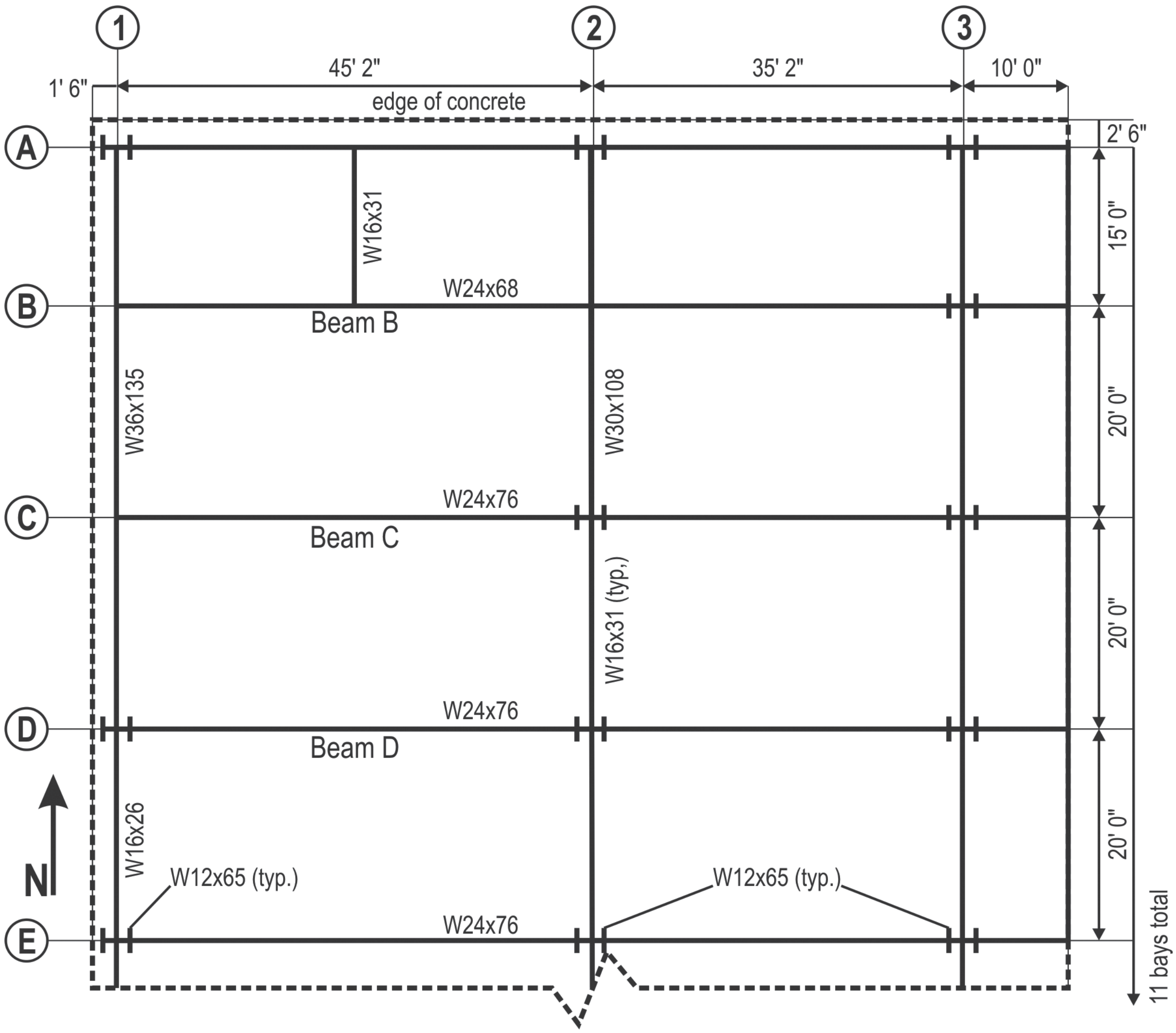

Fig. 2. Test structure steel plan.

one on the top of the bottom flange, and one at the midheight of the web. Gauges are designated by their beam designation and the number 1 through 15, as shown in Figure 4a (e.g., gage D8 is the web midheight gage at midspan of beam D). All gauges were oriented longitudinally to capture flexure-induced strains. The flange gauges were located 1.5 in. from the face of the web so as to avoid both the k-region fillet and the lapping of the deck form (Figure 4b). Strain measurements were taken at various construction milestones and corrected for temperature in accordance with the manufacturer's provided gauge data. All reported data were acquired at ambient temperatures ranging from 38 °F to 52 °F; thus temperature effects were relatively insignificant. "Zero" readings were taken with the bare steel beams supporting only their own self weight and all subsequent data were reported relative to this value. As seen in Figure 4c, form shores were subsequently installed without consideration of the gauges. Where shores bear on the gauges directly, the gauge was damaged and the data not considered in the study.

The fundamental data collected in this work are the longitudinal strains observed at each of the 39 strain gauges. Construction milestones included placement of the concrete, the post-tensioning operation, removal of the shores, and the resulting transfer of the full dead load of the structure to the beam. The milestones are taken as being representative of the stages of the structure's construction and initial operation.

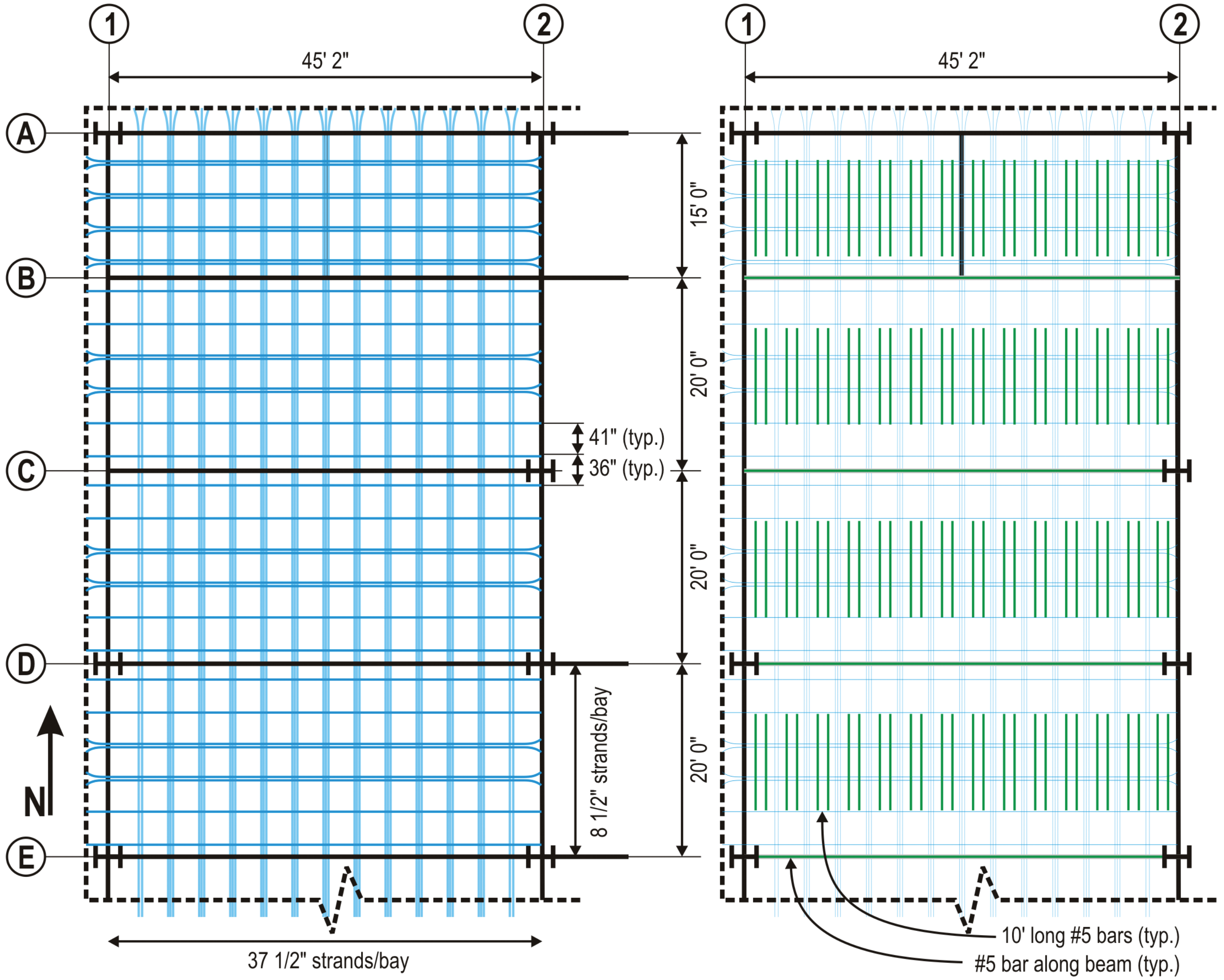

Fig. 3. Test structure slab reinforcement.

All data are provided *relative to the zero readings,* and thus the strains reported do not include the strains associated with the dead load of the beam itself (including some minor construction loads associated with the formwork). Based on a simple span, the maximum stress and strain (in other words, that at midspan) associated with the beam dead load, at the location of the gauges (inside face of flanges), are 1,195 psi and 41 microstrain, respectively. Based on a fixed-fixed span, these values fall to 398 psi and 14 microstrain, respectively. These values have not been added to the data shown because the exact support conditions are uncertain and may vary subtly from beam to beam (Figure 2). The reader is reminded that the top and bottom gage locations are on the insides of the flanges and therefore do not represent the absolute maximum value of strain observed in the steel section.

POST-TENSIONING OPERATION

Post-tensioning of the bay 1-2 slab was conducted when the concrete was five days old. The bay 2-3 slab had not been placed at this time. Concrete strength at the time was 3,450 psi. Tensioning of the secondary strands (i.e., parallel to the beam) began at beam line A and progressed southward along the deck (Figure 2). The ½-in. unbonded strands were pulled from their end along girder line 2 (Figure 1e) with their anchorage 45 ft away at girder line 1. Each strand was pulled to a stress of 216 ksi (0.80 f_{pu}), resulting in an initial strand force of 33,000 lb. Friction and seating losses (ACI, 2005) result in an initial prestress in the tendons following lock-off of approximately 198 ksi (0.73 f_{pu} = 30,200 lb). Long-term losses associated with concrete creep and shrinkage (Aalami, 2004) amount to an additional loss of approximately 9 ksi (0.03 f_{pu}), resulting in a final long-term effective prestress of approximately 189 ksi (0.70 f_{pu}), in the E-W direction. The resulting compressive stress in the concrete in the E-W direction is 160 psi.

Following post-tensioning in the E-W direction, the N-S primary strands were pulled. Based on a stress in the tendon of 0.70 f_{pu}, the resulting concrete stress in the N-S direction following lock-off is approximately 330 psi. In reality, this value is considerably lower due to the length of tendons (approximately 220 ft) and the wobble introduced by the changing slope of the deck and draping of the strand in the N-S direction. Control of the stressing operation was through a

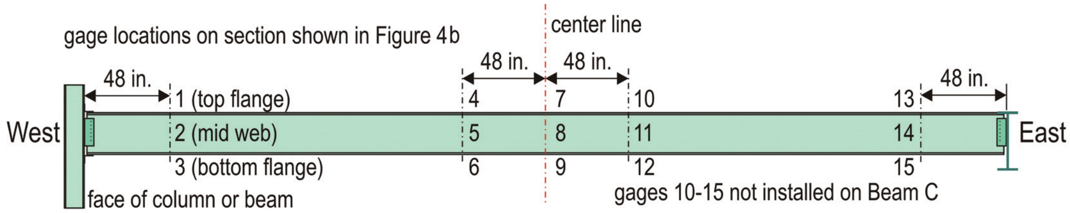

(a) Electrical resistance strain gauge layout along beams B, C and D.

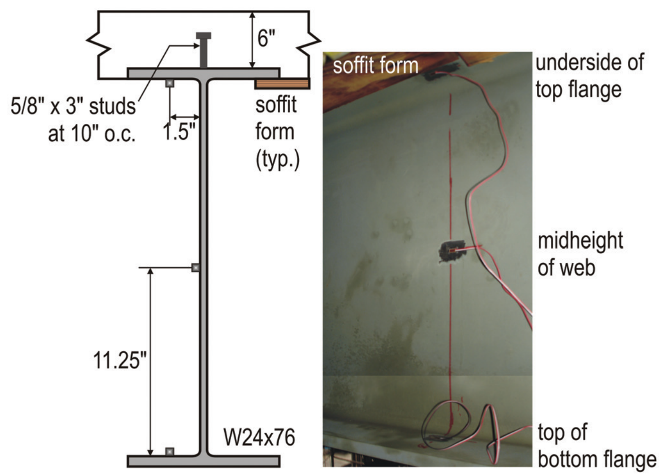

(b) Gauge installation at section.

(c) Gage installation showing form shore installed on top of gauge at this location.

Fig. 4. Instrumentation layout.

pressure-limiting pump operating the stressing jack. Strand elongation—expected to be 3.125 in. in the E-W direction—was also verified at each strand. No moist or accelerated curing techniques were used, which resulted in greater shrinkage losses than are typically expected.

Continuous monitoring of gauges 4, 5 and 6 on beam B and gauges 7, 8 and 9 on beam D was carried out throughout the post-tensioning operation. Gauge readings were recorded at a rate of 1 Hz throughout the operation. Strain-time histories for all six gauges are shown in Figure 5, which shows *relative* strains through the post-tensioning operation. All gauge data was zeroed at 12:50 P.M.—just prior to the initiation of the post-tensioning operation at beam A.

The post-tensioning of the strands immediately above beams B and D occurred at approximately 12:59 P.M. and 1:18 P.M., respectively. In each case approximately one-half of the eventual strain had been developed at these times. It is additionally clear from Figure 5 that only the strands tributary to a girder affect the strain in that girder. It is noted that the "initial condition" of beam D strains in Figure 5 is essentially the same as those of beam B. Little effect from the stressing of beam B (or beam C, between these girders) is apparent in the behavior of beam D. Additionally, despite the observations of Bakota (1988), little effect on the observed beam strains were observed following pulling of the perpendicular (N-S) strands.

LIVE LOAD TESTS

An initial live load test to simply assess the composite behavior of the deck, under full dead load (and to determine the need for a more substantial live load test) was conducted on beam D. In this test, a four-door sedan having specified front and rear GAVW of 1,960 lb and 1,942 lb, respectively, was positioned over the center of Beam D. From the live load strain distribution obtained, the location of the beam neutral axis was determined and the resulting applied moment found. Based on ACI-prescribed design assumptions (composite behavior with an effective slab width, b_{eff} = 105 in.), the maximum observed live load moment is 195,800 lb-in.—this may be interpreted as a lower-bound value. Based on AISC-prescribed design assumptions, the entire tributary slab width is effective (b_{eff} = 240 in.) and the maximum observed live load moment is 212,250 lb-in.—this may be interpreted as an upper-bound value.

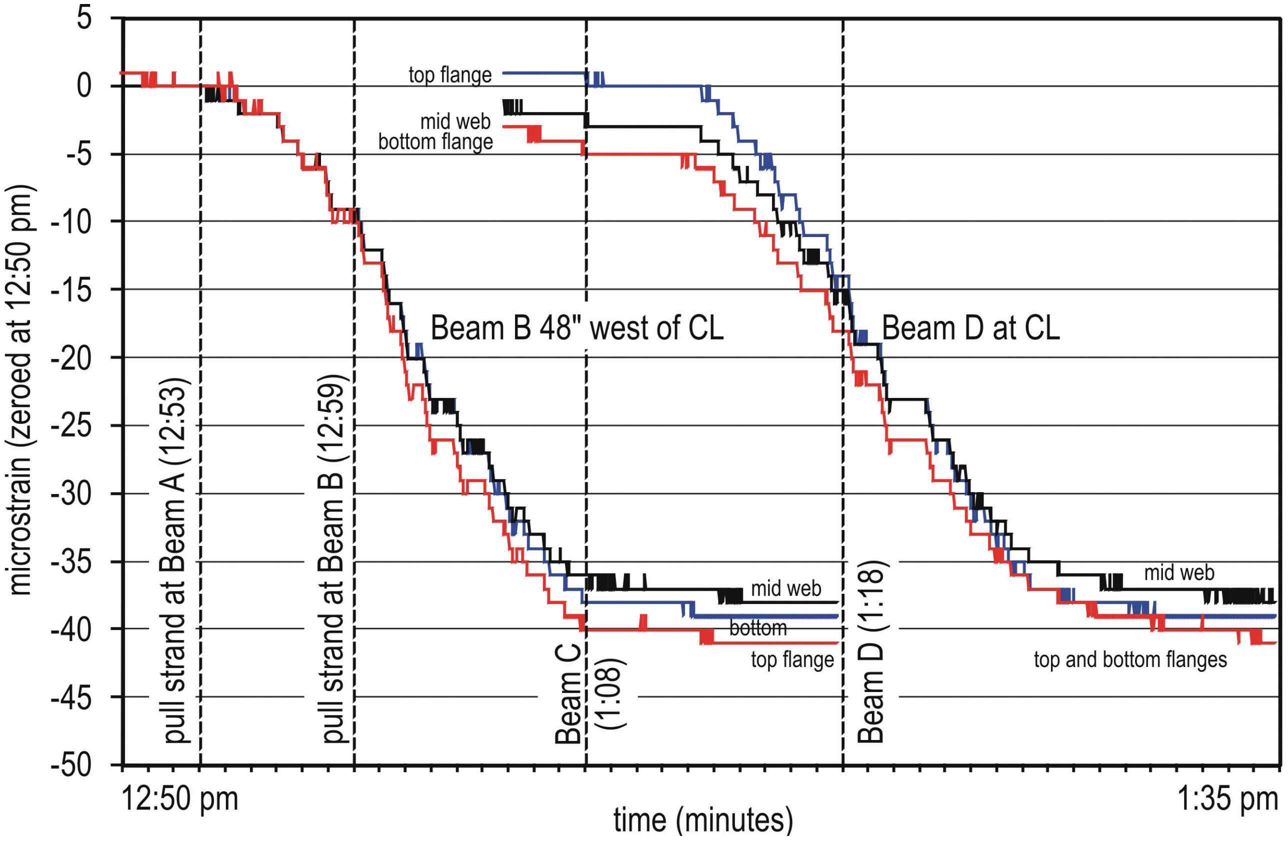

Fig. 5. Strain-time history during post-tensioning operation.

Table 1. Results of Two-Vehicle Live Load Test				
	Assumption	Beam at Midspan (gage 9)		
		B	C	D
Observed tension flange strain (microstrain)		173[a]	42	44
Apparent neutral axis depth[b], y (in.)		[a]	7.0	3.0
Apparent moment (lb-in.)	b_{eff} = 105 in.[c]	[a]	324,000	289,000
Apparent moment (lb-in.)	b_{eff} = 240 in.[d]	[a]	351,800	313,700
Applied moment (lb-in.)	Simply supported	815,500		
Applied moment (lb-in.)	Fixed supports	335,200		

[a] Beam B strain is believed to be an incorrect reading.
[b] Measured from top of 6-in. slab on W24 section.
[c] ACI 318 recommended effective width (see Table 2).
[d] Effective width taken as beam spacing (see Table 2).

The theoretical live load moment resulting from the single vehicle bending case applied is 458,484 lb-in. for a simple span and 203,290 lb-in. for a span having fixed supports. Based on the observed strain behavior, beam D is clearly behaving as a composite member having ends largely restrained from rotation. This result is considered reasonable based on the relatively low stress level applied and the presence of full-depth web angles and partially restrained top and bottom flange angle connections at both ends of beam D.

A second live load test was conducted on all beams. In this test, two vehicles with specified front and rear GAVW of 1,960 lb and 1,942 lb, and 1,714 lb and 1,402 lb, respectively, were positioned over the center of each beam in sequence. The strains resulting only from the application of the live load are given in Table 1. From the live load strain distribution obtained, the location of the beam neutral axis was determined and the resulting applied moment determined. Based on the observed strain behavior and neutral axis locations reported in Table 1, all beams are clearly behaving as composite members having ends largely restrained from rotation.

BEHAVIOR OF STRUCTURAL SYSTEM

Effective Width of Slab

For a steel beam having a composite concrete deck, it is necessary to determine the effective width, b_{eff}, of the flange contributing to the composite beam behavior. For the post-tensioned structure considered, different values of b_{eff} are appropriate for use at different stages of the construction process.

Effective Width While Formwork Is in Place ($b_{eff, form}$)

Between the time that the concrete deck hardens and begins acting compositely with the underlying beams and the time at which the formwork support is removed, a limited portion of the deck slab is able to act in a composite manner with the beam. The formwork supporting the majority of the slab is stiffer in resisting gravity loads than the beam, therefore only that portion of the slab tributary to the beam will affect the load carrying capacity of the beam. In this work, this effective width, $b_{eff, form}$, is taken as 36 in. based on the observed spacing of the formwork in the vicinity of the beams.

Code-Prescribed Effective Width

Only following the removal of the formwork or shores does the beam begin to act in its "designed-for" composite manner. Table 2 gives the code-prescribed values of effective width for both the current AISC and ACI standards. The values given are for beams B, C and D having a 6-in.-deep slab. For design, the value for b_{eff} would be taken as 135 in. (AISC) or 105 in. (ACI). However, design is based on an ultimate load case, in which case some level of slab degradation and cracking is expected. For the dead load and relatively low service load cases considered in this work, the effective width is more appropriately taken as the area tributary to each beam (i.e., b_{eff} = 240 in.). Nonetheless, the selection of effective width has only a marginal effect on the maximum stresses in the steel beam. Considering the range of effective width reported in Table 2, the maximum tensile stress is reduced by only 7% as b_{eff} ranges from 105 in. to 240 in.

Table 2. Effective Width Recommendations		
Parameter	**AISC 2005 Section I3.1a**	**ACI 318-05 Section 8.10.2**
¼ beam span	b_{eff} = 135 in.	b_{eff} = 135 in.
Beam spacing	b_{eff} = 240 in.	n.a.
Clear distance to next web	n.a.	b_{eff} = 240 in.
16 times slab thickness plus beam width	n.a.	b_{eff}f = 105 in.

n.a. = not applicable in cited code document

Table 3. Transformed Section Properties				
Parameter	**Section Behavior**			
	Bare Steel	**Composite at PT Stressing**	**Composite at 28 days**	
Concrete strength, f'_c (psi)	-	3,000	5,000 psi	
Modular ratioa, $n = E_s/E_C$	-	9.3	7.2	
Effective width of slab, b_{eff} (in.)	-	36	135	240
Moment of inertia, I (in.^{4})	2,100	4,651	6,282	6,614
Neutral axis depth (from top of slab), y (in.)	12	10.3	5.5	4.5
Elastic section modulus, top of steel, S_t (in.^{3})	–176	–1,073	12,105	4,424
Elastic section modulus, bottom of steel, S_b (in.^{3})	176	238	257	260
Elastic section modulus, top gage location, S_t* (in.^{3})	–187	–1,272	5,240	3,041
Elastic section modulus, top gage location, S_b* (in.^{3})	187	246	265	268

[a] Ec = 57,000 $\sqrt{f'_c}$; Es = 29,000 ksi

Table 4. Predicted and Observed Behavior at Midspan of Beam D						
Load Case	**Assumed Behavior**	**S_b*[a]**	**Moment**	**Bottom Flange Strain**		**Predicted / Observed**
				Predicted	**Observed**	
		in.^{3}	**lb-in.**	**$\mu\varepsilon$**	**$\mu\varepsilon$**	
Steel self-weight	Noncomposite	187	223,257	41	-	-
Concrete with shores in place[b]	Noncomposite	187	881,616	163	163	1.00
Full concrete dead load[b]	Noncomposite	187	4,612,319	851	ntc	-
Full concrete dead load[b]	Composite b_{eff} = 240 in.	268	4,612,319	593	570	0.96
Single-vehicle live load[c]	Simple support	268	458,484	59	ntc	-
	Fixed supports	268	203,290	26	25	0.96
Two-vehicle live load[c]	Simple support	268	815,500	105	ntc	-
	Fixed supports	268	335,200	43	44	1.02

[a] Elastic section modulus at gage location (see Table 3).
[b] Excludes self weight of steel as this effect is “zeroed” out of observed strains.
[c] Strains due to live load only.
ntc = not the case in test structure—shown for comparison with subsequent table entry.

Predicted Section Behavior

Table 3 provides a summary of composite section properties calculated using different parameters for beams C and D (W24×76 steel section) corresponding to three phases in the structure's construction: bare steel behavior, behavior at post-tensioning, and eventual design behavior (using both the design value of b_{eff} and the beam spacing). An important aspect of behavior shown in this table is the upward migration of the neutral axis location as a greater effective width, b_{eff}, is engaged, and as the concrete strength and modulus increases.

Predicted Behavior of Beam D

Based on the composite section properties presented in Table 3, the expected strain behavior at the midspan of beam D is presented in Table 4. The bottom flange at midspan is chosen for comparison because simple and fixed end moments may be directly compared and the degree of fixity established; and tension flange strains are greater and thus error and noise are proportionally reduced. The length of the beam is taken as 44 ft 2 in.

The predicted behaviors for dead load applications presented in Table 4 are based on *simply supported end conditions* and thus represent upper-bound values. To obtain values for fixed-fixed end conditions for the beam midspan, the tabulated values of midspan moment may be multiplied by 0.33; representing a lower-bound value. The values reported for the live load applications, on the other hand, are presented for both simple and fixed support conditions. In all cases the strains are determined at the gage locations (in other words, using values of S_t* and S_b* from Table 3, as indicated) and E = 29,000 ksi.

In the cases shown in Table 4, the effect of steel dead load is calculated to result in a strain of 41 microstrain. Because data are zeroed based on this value, all subsequent data are reported *relative* to this value; thus it is necessary to add 41 microstrain to all reported values to obtain the actual steel strain. Similarly, the reported live load strains are only those resulting from the application of live load; the dead load strains must be similarly added to these to obtain the actual strain.

The exceptional agreement between predictions based on fundamental assumptions and observed strain data shown in Table 4 illustrates the following aspects of the beam behavior:

1. The assumption of an approximately 36-in. tributary width of fresh concrete being carried by the beam is reasonable ("concrete with shores in place," in Table 4).

2. Dead load is carried primarily in simple bending ("full concrete dead load").

3. The beam behaves as a dominantly fixed ended beam in resisting the relatively small live loads used ("vehicle live load").

The apparent discrepancy between observations 2 and 3 results from the fact that the top and bottom flange angles used where beams frame into columns were not actually tightened at the time of placing the concrete or later removing the forms. It is not clear when and/or if these angles were tightened; however, the presence of the composite slab appeared to stiffen the support conditions by providing a degree of continuity between the beam and supporting girder. This effect, and the low live loads used, should be expected to result in a beam "made continuous for live load" regardless of the presence of flange angles. The observed behavior supports this observation.

A final comment on Table 4 is warranted. The post-tensioning force is introduced after the placement of the concrete and thus should affect all subsequent milestones. However, as will be shown in the following section, the resulting compression strains from the PT forces on the bottom flange of the steel beam are largely "decompressed" (undone) by the PT-induced flexure introduced upon the removal of the shores. As will be shown, this is partially an artifact of the force levels and geometry of the structure considered.

Post-Tension-Induced Stresses

The following discussion is presented in the order in which the post-tensioning operation is carried out and assumes the general scenario whereby the concrete is placed, the post-tensioning is pulled, and then the forms are released.

Post-Tensioning Operation

During the initial post-tensioning operation, the slab remains shored. Axial stresses in the deck system are self-equilibrated resulting in internal stresses associated with the axial force (in other words, the P_i/A component). Flexure-induced stresses associated with the eccentricity of the PT tendons (in other words, the $P_i e/S$ component), however, are largely resisted by the stiff formwork system (recall that the formwork is considerably stiffer than the beam in resisting vertically oriented forces). Thus, only the axial stresses are carried in the beam at the time of post-tensioning. Based on these assumptions, the expected axial strain in the beam and slab due to post-tensioning is 47 microstrain. As reported in Figure 5, the observed axial strain is on the order of 40 microstrain. Factors affecting both the predicted and observed values include (a) the expected variability in concrete properties at an early age and (b) the assumption of 100% composite behavior being developed in carrying axial load. Generally, one would expect the measured steel strains to be lower than the concrete strains. In this light, and based on previous experience, the observations and predictions correlate remarkably well.

Analysis of Post-Tensioning Operation

The assumption promulgated earlier that the post-tensioning operation results in only axial stresses provided the slab remains shored is, admittedly, an idealization. A rigorous analysis of the problem may be made by considering the shored system as a beam on elastic foundations subject to an eccentric axial force producing moments at each end. The elastic foundation, representing the shores, is assigned a stiffness in terms of a unit stress to cause a unit deflection (psi/in., for instance). This stiffness is effectively the axial stiffness of the shoring system resisting vertically applied loads. In general, this stiffness will be relatively large because it effects the vertical deflection of the forms when placing the concrete deck. The shore stiffness has no effect on the axial component of the PT force. The effect of the induced moment is determined based on the behavior of a beam on elastic foundations. Such an analysis is shown schematically in Figure 6.

The midspan moment, M, and vertical deflection, y, due to the PT-induced moment, M_0, may be found to be (Young and Budynas, 2002):

$$M = M_0 \frac{-\cosh\beta\ell\cos\beta\ell}{1+\sinh^2\beta\ell-\sin^2\beta\ell} \tag{1}$$

$$y = \frac{M_0}{2EI\beta^2}\frac{-\sinh\beta\ell\sin\beta\ell}{1+\sinh^2\beta\ell-\sin^2\beta\ell} \tag{2}$$

where

$$\beta = \left(\frac{b_o k_o}{4EI}\right)^{\frac{1}{4}} \tag{3}$$

ℓ = half span of the shored beam
b_o = width of the shored beam
k_o = stiffness of the supporting shores

For the post-tensioned structure considered, the stresses due to the PT-induced moment are negligible provided the shores remain engaged. The midspan moment, $M = 0.014M_0 = -5{,}454$ lb-in., resulting in an extreme tension flange stress of 21 psi and corresponding strain of less than 1 με. Clearly a variety of assumptions can be made in this calculation; the effective stiffness of the beam, I, the actual applied moment, M_0, and the vertical stiffness of the shores, k_0, being the most significant. For the beam geometry considered, however, the extreme tension flange stress calculated based on a wide range of such assumptions did not exceed 10% of the stress due to the axial component of the PT force.

Release of Formwork

Upon the release of the formwork, the PT-induced flexural stresses resulting from the eccentric application of the PT force are transferred from the formwork shores to the beam. At this stage, the concrete has aged further, resulting in a

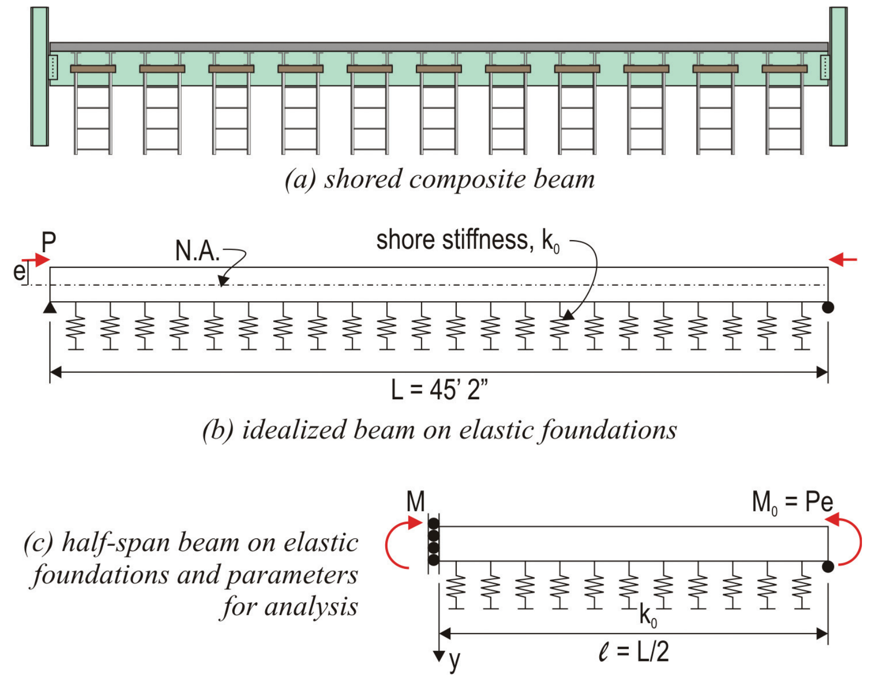

Fig. 6. Schematic representation of shore-supported beam as a beam on elastic foundations.

higher strength and stiffness, which then results in the composite neutral axis migrating upward as the concrete continues to age. If it assumed that the effective width of the slab is 240 in. and the concrete strength has attained a strength of 4,000 psi at the time of formwork release, the additional strain transferred to the bottom flange of the steel beam (at the gage locations) is 50 microstrain. This tensile strain “undoes” the PT-induced axial compressive strain predicted using consistent assumptions to be 47 microstrain.

For the beam and slab geometry considered, the PT-induced flexural strains are approximately 10% of those associated with the transfer of full dead load to the beams (as the forms are released) as shown in Table 4. Additionally, for the geometry considered, the bottom flange strain associated with PT-induced axial force (P_i) and that associated with PT-induced flexure forces (P_ie/S_b) virtually cancel each other. The top flange axial-induced strains are reduced marginally since the neutral axis (in this case) has migrated into the slab.

SUMMARY OF PROCEDURE FOR ASSESSING PT-INDUCED STRESSES

Post-tensioning (PT) forces are introduced to the steel beam-concrete deck system, typically within a week of placing the concrete deck. The concrete deck may be shored (formwork still in place) or unshored when the tensioning operation takes place. The forces resulting from tensioning are resisted by the structural system active at the time of stressing the tendons. If the shores remain in place, the structural system resisting PT-induced forces constitutes the slab, beam and shores. Additionally, the slab-beam composite beam will behave in a composite manner in resisting PT forces to the extent its design permits. That is, where shear studs are provided, the beam will behave in a composite manner with the slab; if studs are not provided, the system will resist forces in a noncomposite manner.

Typically, the unbonded PT tendons will be located at the mid-depth of the slab and will be pulled and anchored in such a manner as to result in concentrated forces being located at the anchorage and pulling ends of the tendon as illustrated in Figure 7. These forces draw the slab into compression and result in an end moment being introduced into the beam. This moment is calculated as the product of the PT force and its lever arm to the neutral axis of the section at the time of tensioning. Thus, the resulting stress in the section is calculated as the sum of the axial and flexural components of the applied PT load, P_i:

$$\sigma_{PT} = P_i/A + (P_ie/S) \tag{4}$$

PT Pulled While Slab Is Shored

If the post-tensioning is pulled while the slab remains shored (Figure 7a), only the PT-induced axial force is transferred to the composite steel beam. The flexural component is primarily resisted by the shores. Thus:

$$\sigma_{PT,\ axial} = P_i/A_{gtr} \tag{5}$$

where

A_{gtr} = gross transformed area of the tributary slab and steel beam composite section determined using the concrete modulus at the time of PT tensioning

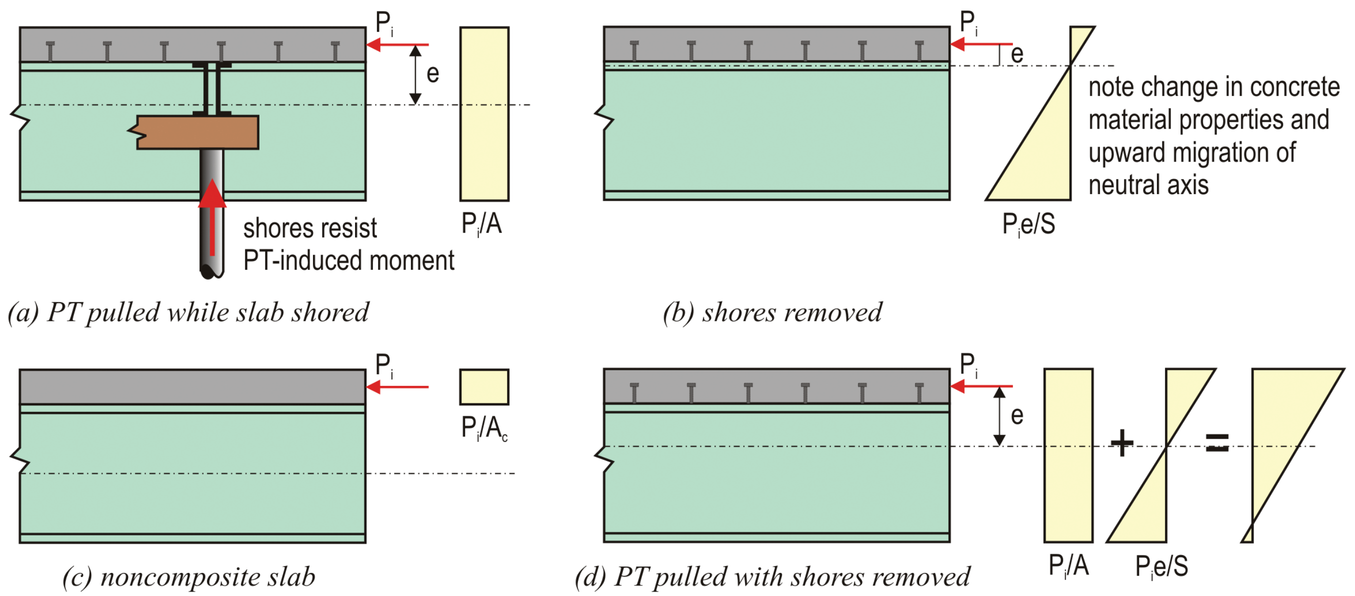

Fig. 7. Effects of post-tensioning forces on members.

Thus a uniform compressive force is applied through the entire composite section (Figure 7a). If the slab is not composite with the beam, this compression is carried only by the slab (Figure 7c). The stiffness of the shoring system may vary; thus a small degree of the PT-induced flexure may be resisted by the beam while the shores are in place. For any reasonable case, however, the extreme tension flange stress due to PT-induced flexure will not exceed 10% of the stress due to the axial component of the PT force while the shores remain engaged.

Once the shores are released (Figure 7b), the PT-induced flexural stresses are transferred to the beam:

$$\sigma_{PT,\,flex} = (P_i e / S) \tag{6}$$

where

e = eccentricity from the tendon centroid to the composite neutral axis

S = appropriate section modulus for the location of interest in the composite section

Both e and S are determined using the concrete modulus at the time of shore release. If the slab is not composite, flexure is only induced in the slab and only if there is an eccentricity in the strands with respect to the slab alone. For most post-tensioned deck applications, the eccentricity will be zero (strand at mid-depth of the slab) and thus no PT-induced flexural stress exists (Figure 7c).

Between the time of PT tensioning (Equation 5) and shore removal (Equation 6), the concrete will age; the modulus will increase resulting in the neutral axis of the composite section migrating upward, reducing the eccentricity, e, in Equation 6.

The net effect of removing the shores after the post-tensioning operation is that the concrete slab compression is increased and the PT-induced axial compression in the tension flange is reduced. Generally, the compression flange is largely unaffected due to its proximity to the neutral axis of the composite beam.

PT Pulled While Slab Is Unshored

This case occurs when the slab forms are supported entirely by the steel beam resulting in an unshored condition throughout the erection process. In this case all PT-induced stresses are carried by the composite beam immediately upon tensioning the strands. In this case, stresses are determined from Equation 4 with all parameters, A, e and S, calculated at the time of PT tensioning (Figure 7d).

Under no circumstances is it possible for the PT-induced flexure to be carried by the noncomposite steel section (Figure 8).

SUMMARY AND CONCLUSIONS

An experimental program of monitoring the during- and post-construction behavior of a steel-framed open parking deck having a cast-in-place post-tensioned concrete slab is presented. Monitoring was carried out following steel erection and ended following completion of the structure. Data were acquired at a variety of stages throughout the construction process. Additionally, two live load tests were conducted. The objective of this field study was to quantitatively assess the effect that slab post-tensioning forces have on their supporting steel members. The following conclusions were drawn:

1. The structure carried its self-weight dead load in a manner consistent with its simply supported design.

2. The relatively small magnitude live loads applied were carried in a fully composite manner with the effective width equal to the beam-to-beam spacing.

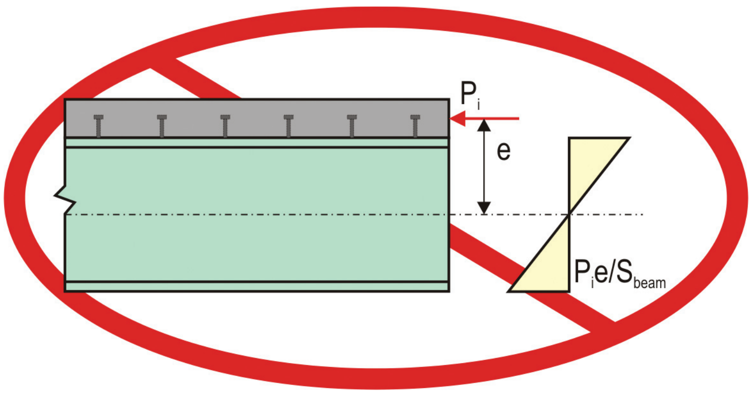

Fig. 8. Under no circumstances can post-tensioning forces be resisted by the steel section alone.

3. While the form shores are in place, the steel beams carry only concrete deck loads tributary to the beam relative to the shores.

4. If shores are in place during the post-tensioning operation, only PT-induced axial stresses are effectively transferred to the supporting steel beams. These stresses may be calculated based on an equivalent transformed gross section analysis.

5. The shores are sufficiently stiff to resist flexural stresses induced by the post-tensioning operation. Once the forms are released, PT-induced flexural stresses are transferred to the supporting steel beam. These stresses should be assessed using a transformed sections analysis and material properties at the time of the form shore release.

6. For the beam and slab geometry considered, the PT-induced flexural strains were approximately 10% of those associated with the transfer of full dead load to the beams (as the forms are released). Additionally, for the geometry considered, the bottom flange strain associated with PT-induced axial force and that associated with flexural forces virtually cancel each other. Resulting in negligible additional stress in the bottom flange of the beam as a result f the two-directional slab post-tensioning. The top flange axial strains are reduced marginally because the neutral axis (in this case) has migrated into the slab.

ACKNOWLEDGMENTS

This study was carried out with support from the American Institute of Steel Construction (AISC). Charles Churches Sr. of Churches Engineering, Washington PA, is the engineer of record for the project. His support and the information he provided is gratefully acknowledged. Eric Campbell of Ionadi Construction, Pittsburgh, PA, was the site supervisor; his assistance was invaluable to the study. The building is owned by Real Estate Enterprises, Pittsburgh, PA; Kai Olander is acknowledged for providing access to the site and test structure. The findings of this work do not necessarily reflect the opinions of those acknowledged here.

REFERENCES

Aalami, B.O. (2004), "Prestressing Losses and Elongation Calculations," *ADAPT, T9-04*, September 2004 (revised October 2004), 16 pp.

ACI (2005), *Building Code Requirements for Structural Concrete*, ACI 318, Farmington Hills, MI.

AISC (2005), *Steel Construction Manual*, 13th ed., American Institute of Steel Construction, Chicago, IL.

Bakota, J.F. (1988), "Parking Structure with a Post-tensioned Deck," *Engineering Journal*, AISC, Third Quarter, pp. 119–125.

Churches, C.H. (2007), personal discussion/correspondence, March.

Churches C.H., Troup, E.W.J. and Angeloff, C. (2003), "Steel-Framed Open-Deck Parking Structures," *Steel Design Guide No. 18*, American Institute of Steel Construction, 113 pp.

Englot, J.M. and Davidson, R.I. (2001), "Steel Framed Parking Garages Take Off at JFK and Newark International Airports," *Modern Steel Construction*, Vol. 44, No. 4, April, 6 pp.

Flynn, L.J. and Astaneh-Asl, A. (2001), "Notes on Design of Steel Parking Structures—Includes Seismic Effects," *Steel Tips*, Structural Steel Education Council.

AISC (1974), "[A] New Structural System for Parking Decks," *Modern Steel Construction*, Vol. 14, No. 2.

Sharma, B. and Harries, K.A. (2007), *Effects of Post-Tensioning on Supporting Beams,* report to AISC, University of Pittsburgh Civil and Environmental Engineering Report No. CE/ST 36, 42 pp.

Simon, A.H. (2001), "Unique Steel Framed Solution to Parking," *Modern Steel Construction*, Vol. 44, No. 4, April, 3 pp.

Sontag, H. (1970), "Steel Multi-Storey Garages," *Acier-Stahl-Steel*, Vol. 35, No. 11, pp 480–490.

Troup, E. and Cross, J. (2003), *Innovative Solutions in Steel: Open-Deck Parking Structures*, American Institute of Steel Construction, Inc., 29 pp.

Young, C.S. and Budynas, R.G. (2002), *Roark's Formulas for Stress and Strain*, 7th ed., McGraw-Hill.